Computational Fluid Dynamics Using a Porous Media Setting Predicts Outcome after Flow-Diverter Treatment

M. Beppu, M. Tsuji, F. Ishida, M. Shirakawa, H. Suzuki, and S. Yoshimura

ABSTRACT

BACKGROUND AND PURPOSE: Knowledge about predictors of the outcome of flow-diverter treatment is limited. The aim of this study was to predict the angiographic occlusion status after flow-diverter treatment with computational fluid dynamics using porous media modeling for decision-making in the treatment of large wide-neck aneurysms.

MATERIALS AND METHODS: A total of 27 patients treated with flow-diverter stents were retrospectively analyzed through computational fluid dynamics using pretreatment patient-specific 3D rotational angiography. These patients were classified into no-filling and contrast-filling groups based on the O'Kelly-Marotta scale. The patient characteristics, morphologic variables, and hemodynamic parameters were evaluated for understanding the outcomes of the flow-diverter treatment.

RESULTS: The patient characteristics and morphologic variables were similar between the 2 groups. Flow velocity, wall shear stress, shear rate, modified aneurysmal inflow rate coefficient, and residual flow volume were significantly lower in the no-filling group. A novel parameter, called the normalized residual flow volume, was developed and defined as the residual flow volume normalized by the dome volume. The receiver operating characteristic curve analyses demonstrated that the normalized residual flow volume with an average flow velocity of ≥8.0 cm/s in the aneurysmal dome was the most effective in predicting the flow-diverter treatment outcomes.

CONCLUSIONS: It was established in this study that the hemodynamic parameters could predict the angiographic occlusion status after flow-diverter treatment.

ABBREVIATIONS: AIRC = aneurysmal inflow rate coefficient; CF = contrast-filling; CFD = computational fluid dynamics; FD = flow diverter; FV = flow velocity; mAIRC = modified aneurysmal inflow rate coefficient; NF = no-filling; nRFV = normalized residual flow volume; RFV = residual flow volume; SR = shear rate; WSS = wall shear stress

Recanalization and retreatment are frequent even after using stent-assisted coil embolization for large wide-neck internal carotid artery aneurysms. The safety and efficacy of the flow diverter (FD) treatment[1,2] have been recently demonstrated in many studies. In the large-scale Pipeline for Uncoilable or Failed Aneurysms study, approximately 76% of the patients had complete aneurysm occlusion on 6-month angiography and 93% had complete aneurysm occlusion on 3-year angiography after treatment.[1,2]

In contrast, some aneurysms need additional treatment and may otherwise rupture. Delayed aneurysm rupture and intraparenchymal hemorrhages are poorly understood and usually lead to fatal complications.[3,4] Rouchaud et al[4] reported that 81.3% of patients with delayed ruptures died or had poor neurologic outcomes and 76.6% of the delayed ruptures occurred within 1 month posttreatment. However, predicting whether an aneurysm would be completely occluded or ruptured after the FD treatment is difficult.

In recent times, the development of computational fluid dynamics (CFD) has enabled the evaluation of hemodynamics of cerebral aneurysms. Umeda et al[5,6] reported the hemodynamic characteristics required to predict the recurrence of coiled aneurysms with CFD using porous media modeling, which can be effective in predicting the postcoiling aneurysm occlusion status. Application of the porous media setting to an intracranial stent may also aid in simulating the hemodynamics after the endovascular treatment with an FD stent.[7]

Received April 11, 2020; accepted after revision July 7.

From the Department of Neurosurgery (M.B., M.S., S.Y.), Hyogo College of Medicine, Hygo, Japan; Department of Neurosurgery (M.T., F.I.), National Hospital Organization Mie Chuo Medical Center, Tsu, Mie, Japan; and Department of Neurosurgery (H.S.), Mie University Graduate School of Medicine, Tsu, Mie, Japan.

Please address correspondence to Mikiya Beppu, PhD, Department of Neurosurgery, Hyogo College of Medicine, 1-1 Mukogawa, Nishinomiya, Hyogo 663-8501, Japan; e-mail: mikiya.beppu@gmail.com

http://dx.doi.org/10.3174/ajnr.A6766

The aim of this study was to evaluate the effectiveness of porous media CFD for predicting the angiographic occlusion status after FD treatment.

MATERIALS AND METHODS

This retrospective study was approved by the institutional ethics committee. The patients provided written informed consent for using their data in this study.

Patient Population and Study Protocol

During 2015–2017, thirty-four unruptured internal carotid artery aneurysms were treated with FD using a Pipeline Embolization Device (Covidien) after 3D rotational angiography.

We evaluated the angiographic occlusion status during follow-up DSA at 6–12 months postprocedure. The DSA findings were classified into 2 groups using the O'Kelly-Marotta classification.[8] We classified the O'Kelly-Marotta classes A (A1, A2, A3), B (B1, B2, B3), and C (C1, C2, C3) as the contrast-filling (CF) group and D as the no-filling (NF) group. Two independent observers who were blinded to the hemodynamic results evaluated and classified the O'Kelly-Marotta grading.

Investigators who were unaware of the occlusion status performed CFD analyses independently. We compared the morphologic variables and hemodynamic parameters of the CF group with those of the NF group. We also evaluated the effectiveness of the CFD analysis for predicting the angiographic occlusion status after FD treatment.

Morphologic Variables

As previously described, the morphologic variables were measured on stereolithographic models generated from preoperative 3D rotational angiography using ImageJ (National Institutes of Health) and CFX-post (CFX CFD19.2; ANSYS).

CFD Analysis

The patient-specific geometries were generated from the DICOM datasets of preoperative 3D rotational angiography that were obtained using Artis zee dBA Twin (Siemens). The surface reconstruction of the computational model was obtained by segmenting the lumen boundary from 3D rotational angiography images using an analytic software (Mimics 16.0; Materialise). The stereolithography was re-meshed to improve the surface triangle quality (3-matic 8.0; Materialise). The 3D neck part was created using a Boolean subtraction between the original geometry and aneurysm-deleted models. A 3D stent domain was obtained by a transformation, in which the 3D neck part was offset by a thickness of 0.048 mm, which corresponded to the diameter of the strut of the Pipeline. The computational hybrid meshes were generated with tetrahedral and prism elements (ICEM CFD19.2; ANSYS). The size of the tetrahedral elements was 0.1–1.2 mm for the fluid domain and 0.05 mm for 3D stent domain. Five prismatic boundary layers with a total thickness of 0.15 mm covered the surface to ensure an accurate definition of the velocity gradient. The average mesh number we used in this study was about 3.8 million. Volumetric meshes were used to ensure sufficient mesh resolution around the 3D stent domain. The effect of mesh density on 3D stent domain controls (the mesh independence study) showed that the mesh size did not remarkably affect hemodynamic parameters evaluated in this study. A straight inlet extension was added to the inlet section to obtain a completely developed laminar flow.

For the fluid domain, the 3D incompressible laminar flow fields were obtained by solving the continuity and Navier–Stokes equations. Numeric modeling was performed using a commercially available CFD package (CFX 19.2; ANSYS). Blood was assumed to be an incompressible Newtonian fluid with a blood density of 1056 kg/m^3 and a blood dynamic viscosity of 0.0035 Pa × s. The typical flow waveform of phase-contrast MR imaging was scaled to achieve the physiologic wall shear stress (WSS).[9,10]

Traction-free boundary conditions were applied at all outlets. When there were several outlets, we set the outlets at a certain distance and height from the aneurysm to prevent uneven distribution of blood flow. The steady-state analysis was performed using the mean flow-volume rate. We used the typical flow waveform of phase-contrast MR imaging to achieve the physiologic WSS based on the Murray law. We used the blood flow rate set by the vessel diameter of the inlet. Thus, the steady flow analysis was assumed to use the mean flow-volume rate.

We conducted the 2-pattern CFD simulations, which involved the simulation of an untreated stent-free aneurysm as the preoperative status (control model) and assuming an aneurysm with a simple placement of an FD stent (FD model) (Fig 1).

FD Model

In this study, we applied the 2 numeric models in the fluid and porous domains. The flow in the fluid domain was simulated using the Navier–Stokes equation and equation of continuity as follows:

$$\nabla \cdot v = div \cdot v = 0,$$

$$\frac{\partial v}{\partial t} + (v \cdot \nabla)v = -\frac{1}{\rho}\nabla p \ + \frac{\mu}{\rho}\nabla^2 v + F,$$

where v is the velocity of the flow, p is the pressure, ρ is the density, μ is the viscosity of the fluid, and F is the body force.

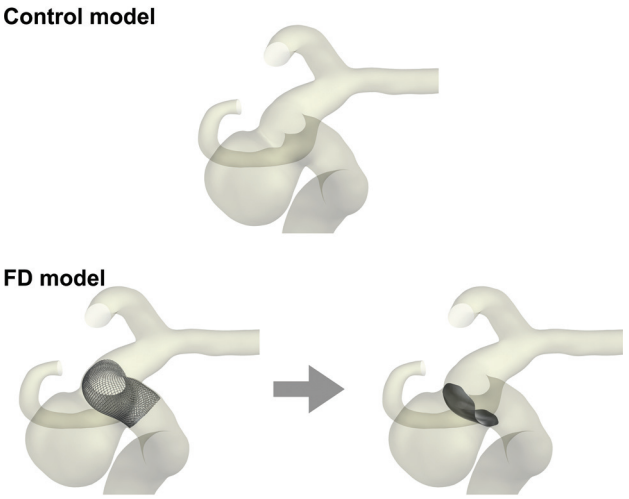

FIG 1. Images of porous media modeling for FD treatment. The control model enables the simulation of preoperative status, whereas the FD model enables the simulation of simple deployment of an FD stent.

Table 1: Comparison of patient characteristics[a]

	CF Group ($n = 11$)	NF Group ($n = 16$)	P Value[b]
Patient characteristics			
Age (yr)	68.6 ± 9.9 (52–83)	61.8 ± 9.7 (40–75)	.09[b]
Male sex	1 (9.1)	1 (6.3)	1.00[c]
Aneurysm characteristics			
Location (cavernous)	2 (18.2)	9 (56.3)	.11[c]
Symptomatic	2 (18.2)	6 (37.5)	.41[c]
Treatment characteristics			
No. of Pipelines	1.0 (1)	1.1 ± 0.3 (1–2)	.42[b]
Coil	0	0	
PTA	1 (9.1)	1 (6.3)	1.00[c]

Note:—CF indicates contrast filling; NF, no filling; PTA, percutaneous transluminal angioplasty.
[a] Data are expressed as mean ± SD (range) or number of cases (% of cases).
[b] P values were estimated using the Welch t test between CF and NF groups.
[c] P values were estimated using Fisher exact tests or χ^2 tests between CF and NF groups.

The flow in the stent regimes was simulated using porous media modeling that follows the Darcy law. In these flow regimes, pressure was locally balanced with resistance forces, such that

$$0 = -\nabla p - K\nu,$$

where K is a constant of porous resistance. This was assumed to be a quasilinear function of the magnitude of velocity,

$$K = \alpha v + \beta,$$

where α and β are coefficients, for which the values are determined using the Ergun equation as follows:

$$\alpha = \frac{1.75\rho(1-\kappa)}{\kappa^3 D_P}$$

$$\beta = \frac{150\mu(1-\kappa)^2}{\kappa^3 D_P^2},$$

where D_P is the average particle diameter.[11] It was set to 0.048 mm, which corresponded to the diameter of the strut of the Pipeline.

The volume coverage ratio is defined as the ratio of the volume of the stent strut to the stent volume. The variable κ[12] denotes the porosity of the porous media stent.

$$Volume\ Coverage\ Ratio\ (\%) = \frac{Volume\ of\ Stent\ Strut}{Stent\ Volume} \times 100$$

$$\kappa(Stent) = 1 - \frac{Volume\ Coverage\ Ratio}{100}.$$

The metal coverage ratio is defined as the ratio of the area of the stent strut to the stent area. The relationship between the volume coverage ratio and metal coverage ratio is defined using the following formula:

$$Volume\ Coverage\ Ratio = \frac{\pi}{6} \times Metal\ Coverage\ Ratio.$$

The metal coverage ratio of the Pipeline was considered to be approximately 30%. Thus, we estimated the volume coverage ratio as 15%. In an aneurysm treated by overlapping 2 FDs, the volume coverage ratio was assumed to be 30% for aneurysmal flow reduction. To simulate the hemodynamics in an occlusion status, we calculated hemodynamic parameters under steady-state conditions. The aneurysmal inflow rate coefficient (AIRC) was used as a predictor of recanalization after coil embolization in basilar tip aneurysms.[13] The original AIRC is the proportion of the aneurysmal inflow rate to the basilar artery flow rate. We modified this parameter for internal carotid artery aneurysms, and the modified AIRC (mAIRC) denoted the proportion of the aneurysmal inflow rate to the proximal parent artery flow rate.

The residual flow volume (RFV) was calculated to predict the postcoiling angiographic results in unruptured cerebral aneurysms.[5,6] The RFV was the volume of fluid domain in the aneurysmal dome and was defined as the volume with more than the following mean flow velocity (FV): Tested thresholds included 4, 6, 8, 10, 12, 14, 16, 18, and 20 cm/s. Because RFV was affected by the volume of aneurysmal dome, we developed a novel parameter, the normalized residual flow volume (nRFV), which is defined as RFV normalized by the dome volume. The nRFVα denoted nRFV with an average FV of over α cm/s. We calculated the mAIRC in the control model, RFV in the FD model, and FV, WSS, and shear rate (SR) in both models.

Statistical Analysis

All values were expressed as mean ± SD. Statistical analyses were performed using the software environment R (Version 3.3.3; http://www.r-project.org/). We compared the variables between the CF and NF groups using the Welch t test. P values $< .05$ were considered statistically significant, while the area under the receiver operating characteristic curve was used to determine the diagnostic accuracy of predicting intra-aneurysmal thrombosis.

RESULTS

Among the 34 patients, 7 were excluded because of the difficulty in reconstructing the vascular geometry from 3D rotational angiography. Therefore, 27 patients with 27 unruptured aneurysms, which were treated endovascularly with an FD stent, fulfilled the criteria and constituted the study population. The patients' characteristics, aneurysm characteristics, and treatment characteristics in the 2 groups are summarized in Table 1.

Differences between the NF and CF Groups on Univariate Analyses

Patient Characteristics and Aneurysmal Morphologic Variables. No significant differences were observed in terms of patient characteristics and aneurysmal morphologic variables between the NF and CF groups (Tables 1 and 2).

Aneurysmal Hemodynamic Factors. Among the hemodynamic parameters in the control CFD, FV (0.16 m/s versus 0.28 m/s;

Table 2: Comparison of morphologic variables[a]

Morphologic Variables	CF Group ($n = 11$)	NF Group ($n = 16$)	*P* Value[b]
Aneurysm depth (mm)	6.72 ± 2.26 (3.52–11.04)	6.33 ± 2.28 (3.45–11.87)	.67
Projection length (mm)	6.79 ± 2.29 (3.60–11.25)	6.84 ± 2.31 (3.50–11.96)	.96
Maximum size (mm)	12.67 ± 4.60 (9.41–25.49)	12.98 ± 4.97 (7.74–23.27)	.87
Neck width (mm)	11.72 ± 4.07 (9.14–23.32)	11.56 ± 4.84 (6.14–22.61)	.93
Parent artery diameter (mm)	5.13 ± 0.50 (4.14–5.89)	5.06 ± 0.61 (4.02–6.56)	.74
Aspect ratio	0.59 ± 0.16 (0.37–0.91)	0.61 ± 0.27 (0.31–1.11)	.79
Projection ratio	0.59 ± 0.16 (0.38–0.91)	0.65 ± 0.25 (0.33–1.12)	.50
Size ratio	2.51 ± 1.00 (1.67–5.17)	2.59 ± 1.02 (1.52–4.92)	.83
Neck area (cm^2)	0.99 ± 0.76 (0.56–3.21)	0.92 ± 0.69 (0.27–2.51)	.80
Dome area (cm^2)	2.57 ± 1.84 (1.05–7.47)	2.29 ± 1.46 (0.90–5.11)	.68
Dome volume (cm^2)	0.58 ± 0.68 (0.13–2.51)	0.46 ± 0.43 (0.10–1.35)	.61
VOR (mm)	5.13 ± 2.36 (2.32–9.38)	4.96 ± 2.65 (2.04–11.00)	.86

Note:—VOR indicates volume-to-osmium area ratio.
[a] Data are expressed as mean ± SD (range).
[b] *P* values were estimated using the Welch *t* test between CF and NF groups.

Table 3: Comparison of hemodynamic parameters[a]

Hemodynamic Parameters	CF Group ($n = 11$)	NF Group ($n = 16$)	*P* Value[b]
Control model			
$FV_{aneurysm}$ (m/s)	0.27 ± 0.08 (0.12–0.43)	0.16 ± 0.08 (0.03–0.31)	.003
WSS (Pa)	4.66 ± 1.89 (1.27–7.89)	2.92 ± 1.87 (0.40–7.16)	.03
SR ($\times 10^2$/s)	12.83 ± 5.2 (2.78–21.68)	8.12 ± 5.10 (1.13–19.22)	.03
mAIRC	0.29 ± 0.19 (0.11–0.70)	0.14 ± 0.09 (0.02–0.34)	.04
FD model			
$FV_{aneurysm}$ (m/s)	0.16 ± 0.03 (0.10–0.23)	0.10 ± 0.05 (0.01–0.20)	.002
WSS (Pa)	1.00 ± 0.31 (0.52–1.59)	0.67 ± 0.45 (0.01–1.39)	.03
SR (1/s)	10.55 ± 3.1 (5.73–16.60)	7.22 ± 4.74 (0.14–14.70)	.03

Note:—$FV_{aneurysm}$ indicates average flow velocity in the aneurysmal dome.
[a] Data are expressed as mean ± SD (range).
[b] *P* values were estimated using the Welch *t* test between CF and NF groups.

Table 4: Comparison of RFV and nRFV[a]

Parameters	CF Group ($n = 11$)	NF Group ($n = 16$)	*P* Value[b]
RFV_4 (mm^3)	553.4 ± 616.5 (128.4–2264.0)	358.9 ± 358.5 (0–1307.0)	.42
RFV_6 (mm^3)	526.3 ± 552.9 (123.5–2036.0)	331.8 ± 338.0 (0–1230.0)	.31
RFV_8 (mm^3)	495.8 ± 486.9 (118.6–1800.0)	262.5 ± 290.1 (0–1070.0)	.18
RFV_{10} (mm^3)	454.9 ± 406.1 (111.0–1519.0)	210.8 ± 259.9 (0–913.2)	.10
RFV_{12} (mm^3)	399.5 ± 304.1 (103.6–1174.0)	175.2 ± 229.6 (0–753.6)	.05
RFV_{14} (mm^3)	329.7 ± 201.5 (93.9–833.0)	140.1 ± 196.3 (0–586.2)	.02
RFV_{16} (mm^3)	250.6 ± 119.5 (82.7–463.3)	110.2 ± 159.8 (0–526.4)	.02
RFV_{18} (mm^3)	181.5 ± 99.2 (67.7–406.4)	84.4 ± 124.6 (0–432.3)	.03
RFV_{20} (mm^3)	142.9 ± 106.7 (27.7–382.3)	58.3 ± 85.8 (0–292.0)	.04
$nRFV_4$	0.97 ± 0.02 (0.90–0.99)	0.84 ± 0.27 (0–0.99)	.07
$nRFV_6$	0.95 ± 0.05 (0.81–0.98)	0.77 ± 0.29 (0–0.97)	.02
$nRFV_8$	0.92 ± 0.07 (0.72–0.97)	0.64 ± 0.33 (0–0.96)	.004
$nRFV_{10}$	0.88 ± 0.10 (0.61–0.96)	0.54 ± 0.37 (0–0.95)	.002
$nRFV_{12}$	0.82 ± 0.14 (0.47–0.94)	0.46 ± 0.37 (0–0.93)	.001
$nRFV_{14}$	0.74 ± 0.20 (0.33–0.92)	0.37 ± 0.34 (0–0.90)	.001
$nRFV_{16}$	0.64 ± 0.26 (0.19–0.90)	0.29 ± 0.31 (0–0.85)	.004
$nRFV_{18}$	0.53 ± 0.30 (0.07–0.87)	0.24 ± 0.28 (0–0.79)	.02
$nRFV_{20}$	0.43 ± 0.31 (0.03–0.82)	0.17 ± 0.23 (0–0.71)	.03

Note:—RFV_4, RFV_6, RFV_8, RFV_{10}, RFV_{12}, RFV_{14}, RFV_{16}, RFV_{18}, and RFV_{20} indicate intra-aneurysmal RFV with an average flow velocity of >4, 6, 8, 10, 12, 14, 16, 18, and 20 cm/s, respectively; and $nRFV_4$, $nRFV_6$, $nRFV_8$, $nRFV_{10}$, $nRFV_{12}$, $nRFV_{14}$, $nRFV_{16}$, $nRFV_{18}$, and $nRFV_{20}$ indicate intra-aneurysmal nRFV with an average flow velocity of >4, 6, 8, 10, 12, 14, 16, 18, and 20 cm/s, respectively.
[a] Data are expressed as mean ± SD (range).
[b] *P* values were estimated using the Welch *t* test between CF and NF groups.

$P = .003$), WSS (2.92 Pa versus 4.66 Pa; $P = .03$), SR (8.12×10^2 1/s versus 12.83×10^2 1/s; $P = .03$), and the mAIRC (0.14 versus 0.29; $P = .04$) were significantly lower in the NF group (Table 3).

The porous media CFD showed that FV (0.10 m/s versus 0.16 m/s; $P = .002$), WSS (0.67 Pa versus 1.00 Pa; $P = .03$), SR (7.22×10^2 1/s versus 10.55×10^2 1/s; $P = .03$), RFV_{14} (140.1 mm^3 versus 329.7 mm^3; $P = .02$), RFV_{16} (110.2 mm^3 versus 250.6 mm^3; $P = .02$), RFV_{18} (84.4 mm^3 versus 181.5 mm^3; $P = .03$), and RFV_{20} (58.3 mm^3 versus 142.9 mm^3; $P = .04$) were significantly lower in the NF group than in the CF group (Tables 3 and 4). Similar findings were observed for $nRFV_6$ (0.77 versus 0.95; $P = .02$), $nRFV_8$ (0.64 versus 0.92; $P = .004$), $nRFV_{10}$ (0.54 versus 0.88; $P = .002$), $nRFV_{12}$ (0.46 versus 0.82; $P = .001$), $nRFV_{14}$ (0.37 versus 0.74; $P = .001$), $nRFV_{16}$ (0.29 versus 0.64; $P = .004$), $nRFV_{18}$ (0.24 versus 0.53; $P = .02$), and $nRFV_{20}$ (0.17 versus 0.43; $P = .03$) (Table 4).

Receiver Operating Characteristic Curve Analyses of Possible Determinants for Intra-Aneurysmal Thrombosis after FD Treatment

Among the parameters that demonstrated significant differences between the CF and NF groups on univariate analyses, $nRFV_8$ demonstrated the highest area under the receiver operating

Table 5: ROC curve analysis for hemodynamic parameters that had significant differences between the CF and NF groups on univariate analyses to predict intra-aneurysmal thrombosis after FD treatment

	AUC	95% CI	Sensitivity	Specificity	Cutoff Value
Control model					
$FV_{aneurysm}$	0.82	0.66–0.98	0.81	0.73	0.24 m/s
WSS	0.77	0.58–0.95	0.75	0.73	3.76 Pa
SR	0.76	0.56–0.95	0.75	0.73	1053.0 1/s
mAIRC	0.77	0.59–0.95	0.50	1.00	0.10
FD model					
$FV_{aneurysm}$	0.82	0.66–0.98	0.75	0.82	0.14 m/s
WSS	0.71	0.51–0.91	0.44	1.00	0.42 Pa
SR	0.71	0.51–0.91	0.44	1.00	449.0 1/s

Note:—AUC indicates area under the ROC curve; ROC, receiver operating characteristic.

Table 6: ROC curve analysis for RFV and nRFV that had significant differences between the CF and NF groups on univariate analyses to predict intra-aneurysmal thrombosis after FD treatment

	AUC	95% CI	Sensitivity	Specificity	Cutoff Value
RFV_{14}	0.81	0.64–0.99	0.81	0.82	141.0 mm^3
RFV_{16}	0.81	0.64–0.99	0.75	0.91	100.9 mm^3
RFV_{18}	0.76	0.57–0.95	0.56	1.00	23.8 mm^3
RFV_{20}	0.79	0.62–0.96	0.56	1.00	15.7 mm^3
$nRFV_6$	0.84	0.69–0.99	0.75	0.82	0.95
$nRFV_8$	0.85	0.71–1.00	0.88	0.73	0.93
$nRFV_{10}$	0.83	0.67–0.99	0.81	0.73	0.86
$nRFV_{12}$	0.82	0.65–0.98	0.81	0.82	0.76
$nRFV_{14}$	0.82	0.66–0.99	0.81	0.82	0.66
$nRFV_{16}$	0.82	0.65–0.98	0.81	0.82	0.58
$nRFV_{18}$	0.79	0.62–0.96	0.63	0.82	0.19
$nRFV_{20}$	0.78	0.61–0.96	0.50	1.00	0.03

Note:—RFV_{14}, RFV_{16}, RFV_{18}, and RFV_{20} indicate intra-aneurysmal RFV with an average flow velocity of >14, 16, 18. 20 cm/s, respectively; and $nRFV_6$, $nRFV_8$, $nRFV_{10}$, $nRFV_{12}$, $nRFV_{14}$, $nRFV_{16}$, $nRFV_{18}$, and $nRFV_{20}$ indicate intra-aneurysmal nRFV with an average flow velocity of >6, 8, 10, 12, 14, 16, 18, and 20 cm/s, respectively.

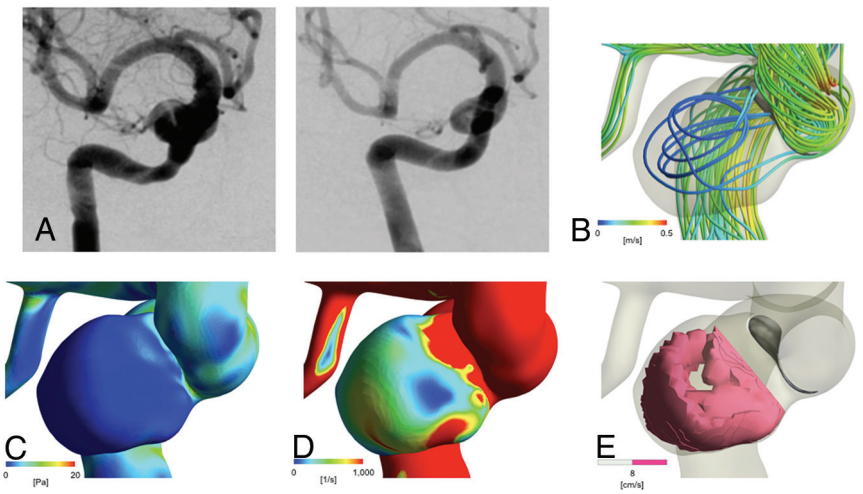

FIG 2. Representative no-filling case. A 58-year-old woman with an asymptomatic aneurysm. *A*, Digital subtraction angiography shows a large wide-neck aneurysm located at the left cavernous portion of the internal carotid artery (*left*), which completely disappeared 6 months after the FD treatment (*right*). *B*, Streamline of FV in the FD model. The mean FV at the dome is 0.06 m/s. *C*, Contour line of wall shear stress in the FD model (mean value at the dome is 0.37 Pa). *D*, Contour line of the shear rate in the FD model (mean value at the dome is 3.96 $\times 10^2$ 1/s). *E*, Intra-aneurysmal nRFV of 0.38 with an average flow velocity of >8 cm/s.

characteristic curve value of 0.85 (95% CI, 0.71–1.00). The cutoff value was 0.93 with a sensitivity of 0.88 and a specificity of 0.73 (Tables 5 and 6).

Representative Cases

Case 1: NF. A 58-year-old woman had a left cavernous portion aneurysm (Fig 2). The maximum size and neck width were 10.1 and 7.7 mm, respectively. In the control model, FV, WSS, SR, and the mAIRC were 0.08 m/s, 1.13 Pa, 3.20 $\times$ 10^2 1/s, and 0.02, respectively. In the FD model, FV, WSS, and SR were 0.06 m/s, 0.37 Pa, and 3.96 $\times$ 10^2 1/s, respectively. RFV_{16} and $nRFV_8$ were 11.1 mm^3 and 0.38, respectively. We treated this aneurysm with FD using a Pipeline Embolization Device (4.5 $\times$ 20 mm). DSA at 6 months after treatment showed complete disappearance of the aneurysm.

Case 2: CF. A 73-year-old woman had a left paraclinoid-portion aneurysm (Fig 3). The maximum size and the neck width were 12.4 and 11.7 mm, respectively. In the control model, the values of FV, WSS, SR, and the mAIRC were 0.43 m/s, 7.89 Pa, 21.68 $\times$ 10^2 1/s, and 0.54, respectively. In the FD model, FV, WSS, and SR were 0.22 m/s, 1.25 Pa, and 12.8 $\times$ 10^2 1/s, respectively. RFV_{16} and $nRFV_8$ were 429.0 mm^3 and 0.96, respectively. We treated this aneurysm with a FD using a Pipeline Embolization Device (4.75 $\times$ 25 mm). The DSA at 6 months after treatment showed an incomplete disappearance of the aneurysm.

DISCUSSION

In this study, we demonstrated that the hemodynamic parameters using both control CFD and porous media CFD could predict the angiographic occlusion status at 6 months after the FD treatment. In addition, $nRFV_8$ was the strongest predictor. These results indicated that preoperative CFD could be effective in decision-making during the treatment of large wide-neck internal carotid artery aneurysms.

A previous CFD study with high-fidelity virtual stent placement showed that posttreatment aneurysmal flow reduction, including the average FV, WSS, inflow rate, and turnover time,

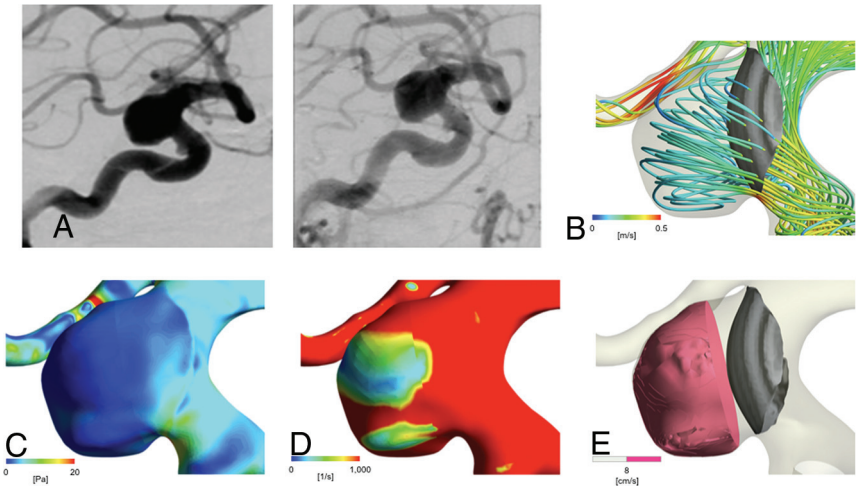

FIG 3. Representative contrast-filling case. A 73-year-old woman with an asymptomatic aneurysm. *A*, Digital subtraction angiography shows a large wide-neck aneurysm located at the left paraclinoid portion of internal carotid artery (*left*), which does not disappear at 6 months after the FD treatment (*right*). *B*, Streamline of FV in the FD model. The mean FV at the dome is 0.22 m/s. *C*, Contour line of wall shear stress in the FD model (mean value in the dome is 1.25 Pa). *D*, Contour line of the shear rate in the FD model (mean value in the dome is 12.8×10^2 1/s). *E*, Intra-aneurysmal nRFV of 0.96 with an average flow velocity of >8 cm/s.

could be correlated with aneurysmal occlusion outcomes.[14] In the in vivo studies, local FV and SR were significantly smaller and the mean transit time was higher in occluded aneurysms than in the rest of the cases.[15] These results suggested that hemodynamic reduction in terms of FV, SR, and WSS is the most important mechanism to induce intra-aneurysmal thrombosis. Corbett et al[16] reported that flow-induced thrombosis occurred under an SR threshold of 54 seconds^{-1} or a specific WSS threshold of 0.41 Pa. These in vivo and in vitro results support the findings of the present study.

We also demonstrated that the NF group had significantly lower mAIRC and RFV values. These results were similar to those reported by Sugiyama et al[13] and Umeda et al.[5,6] Sugiyama et al stated that the AIRC was an independent and significant predictor for recanalization after coil embolization. Umeda et al reported that RFV was an effective parameter in predicting the recurrence of coiled aneurysms. It was suggested that mAIRC and RFV could be good predictors for the angiographic occlusion status after the FD treatment, as in the case of coil embolization.[5,6,13] In this study, the receiver operating characteristic curve analyses demonstrated that $nRFV_{8.0}$ had the strongest predictive capability among all studied parameters.

The clinical implication of the present study is the ability to predict whether the FD treatment is effective for every individual case. Mut et al[17] demonstrated that the aneurysms in the fast occlusion group demonstrated a lower mean FV, inflow rate, and SR. However, these values were determined under posttreatment hemodynamic conditions. Therefore, it remains unknown whether their findings could be used for treatment decision-making. In contrast, the FV at an aneurysm dome using a porous media setting can simulate the outcomes of selected reconstructive treatments, such as direct operations with respect to trapping of an aneurysm and parent artery with high-flow bypass and FD treatment with/without coils.

To treat an aneurysm with insufficient FV reduction by endovascular treatment, we considered the following 2 treatments to increase the reduction of FV. The first approach involves FD stent placement with coils. In a previous study, it was demonstrated that the FD treatment with coils further reduced FV and WSS and increased the low wall shear area.[18] Double-porous media CFD can be used to predict the post-treatment angiographic aneurysmal occlusion status preoperatively.[19] The other approach involves overlapping FD stents or performing compacted FD stent placement. Some reports showed that overlapped or compacted FD stents reduced the values of hemodynamic parameters, including the mean intra-aneurysmal FV, WSS, and inflow rate.[20] Therefore, FD stent placement with coils, overlapped FD stent placement, and compacted FD stent placement can be considered as treatment options for aneurysms with insufficient FV reduction.

The present study has several limitations. First, this study is simple and retrospective. A prospective larger cohort study that includes all types of aneurysms is required to establish the effectiveness of hemodynamic simulation for predicting the outcome of the FD treatment. Second, all the patients who participated in the study were Japanese. Some studies indicated that there was a racial difference in platelet function.[21] They suggested that ethnicity might be an important factor in determining the outcome of the FD treatment. Third, other factors could influence the outcome of the FD treatment, including body forces such as blood viscosity and blood pressure, antiplatelet effect, aneurysm location, branching artery, and incomplete FD expansion. It is difficult for this model to accurately reflect the stent-placement conditions that can influence the hemodynamic factors, but this model makes a distribution of stent uniform.

In addition, we cannot overlook the limitations of the CFD studies. The vessel walls were assumed to be rigid, and blood was modeled as a Newtonian fluid in this study. Newtonian fluids may overestimate WSS and SR at the aneurysmal dome.[22] Therefore, our quantitative CFD results might have some bias. Further studies are thus necessary to validate the results under different simulations.

CONCLUSIONS

All studied hemodynamic factors were significantly lower in the NF group, and $nRFV_8$ was observed to be the strongest predictor of aneurysmal occlusion status after the FD treatment. It was shown that CFD could be useful in pretreatment planning, thereby contributing to more reliable and effective FD treatments for cerebral aneurysms.

ACKNOWLEDGMENTS

We thank Editage (www.editage.jp) for English language review of the manuscript.

Disclosures: Manabu Shirakawa—*UNRELATED*: *Payment for Lectures Including Service on Speakers Bureaus*: Stryker, *Comments*: lecture fee. Shinichi Yoshimura—*RELATED*: *Consulting Fee or Honorarium*: Medtronic, *Comments*: lecture fee; *UNRELATED*: *Consultancy*: Kaneka Medix; *Payment for Lectures Including Service on Speakers Bureaus*: Boehringer Ingelheim, Daiichi Sankyo, Bayer Yakuhin, Ltd. Bristol-Meyers Squibb, Stryker, Sanofi, Otsuka Pharmaceutical, Johnson & Johnson, MicroVention Terumo, Biomedical Solutions.

REFERENCES

1. Becske T, Potts MB, Shapiro M, et al. **Pipeline for uncoilable or failed aneurysms: 3-year follow-up results**. *J Neurosurg* 2017;127:81–88 CrossRef Medline
2. Becske T, Brinjikji W, Potts MB, et al. **Long-term clinical and angiographic outcomes following Pipeline embolization device treatment of complex internal carotid artery aneurysms: five-year results of the Pipeline for Uncoilable or Failed Aneurysms Trial**. *Neurosurgery* 2017;80:40–48 CrossRef Medline
3. Cruz JP, Chow M, O'Kelly C, et al. **Delayed ipsilateral parenchymal hemorrhage following flow diversion for the treatment of anterior circulation aneurysms**. *AJNR Am J Neuroradiol* 2012;33:603–08 CrossRef Medline
4. Rouchaud A, Brinjikji W, Lanzino G, et al. **Delayed hemorrhagic complications after flow diversion for intracranial aneurysms: a literature overview**. *Neuroradiology* 2016;58:171–77 CrossRef Medline
5. Umeda Y, Ishida F, Tsuji M, et al. **Computational fluid dynamics (CFD) analysis using porous media modeling predicts angiographic occlusion status after coiling of unruptured cerebral aneurysms: preliminary study**. *Journal of Neuroendovascular Therapy* 2015;9:69–77 CrossRef
6. Umeda Y, Ishida F, Tsuji M, et al. **Computational fluid dynamics (CFD) using porous media modeling predicts recurrence after coiling of cerebral aneurysms**. *PLoS One* 2017;12:e0190222 CrossRef Medline
7. Li Y, Zhang M, Verrelli DI, et al. **Numerical simulation of aneurysmal haemodynamics with calibrated porous-medium models of flow-diverting stents**. *J Biomech* 2018;80:88–94 CrossRef Medline
8. O'Kelly CJ, Krings T, Fiorella D, et al. **A novel grading scale for the angiographic assessment of intracranial aneurysms treated using flow diverting stents**. *Interv Neuroradiol* 2010;16:133–37 CrossRef Medline
9. Murray CD. **The physiological principle 1 of minimum work applied to the angle of branching of arteries**. *J Gen Physiol* 1926;9:835–41 CrossRef Medline
10. Ford MD, Alperin N, Lee SH, et al. **Characterization of volumetric flow rate waveforms in the normal internal carotid and vertebral arteries**. *Physiol Meas* 2005;26:477–88 CrossRef Medline
11. Akgiray Ö, Saatçı AM. **A new look at filter backwash hydraulics**. *Water Science & Technology: Water Supply* 2001;1:65–72 CrossRef
12. Derdeyn CP, Chimowitz MI, Lynn MJ, et al; Stenting and Aggressive Medical Management for Preventing Recurrent Stroke in Intracranial Stenosis Trial Investigators. **Aggressive medical treatment with or without stenting in high-risk patients with intracranial artery stenosis (SAMMPRIS): the final results of a randomised trial**. *Lancet* 2014;383:333–41 CrossRef Medline
13. Sugiyama S, Niizuma K, Sato K, et al. **Blood flow into basilar tip aneurysms: a predictor for recanalization after coil embolization**. *Stroke* 2016;47:2541–47 CrossRef Medline
14. Xiang J, Damiano RJ, Lin N, et al. **High-fidelity virtual stenting: modeling of flow diverter deployment for hemodynamic characterization of complex intracranial aneurysms**. *J Neurosurg* 2015;123:832–40 CrossRef Medline
15. Chung B, Mut F, Kadirvel R, et al. **Hemodynamic analysis of fast and slow aneurysm occlusions by flow diversion in rabbits**. *J Neurointerv Surg* 2015;7:931–35 CrossRef Medline
16. Corbett SC, Ajdari A, Coskun AU, et al. **In vitro and computational thrombosis on artificial surfaces with shear stress**. *Artif Organs* 2010;34:561–69 CrossRef Medline
17. Mut F, Raschi M, Scrivano E, et al. **Association between hemodynamic conditions and occlusion times after flow diversion in cerebral aneurysms**. *J Neurointerv Surg* 2015;7:286–90 CrossRef Medline
18. Jing L, Zhong J, Liu J, et al. **Hemodynamic effect of flow diverter and coils in treatment of large and giant intracranial aneurysms**. *World Neurosurg* 2016;89:199–207 CrossRef Medline
19. Tsuji M, Kishimoto T, Tomoyuki K, et al. **Double porous media modeling in computational fluid dynamics for hemodynamics of stent-assisted coiling of intracranial aneurysms: A technical case report**. *Brain Hemorrhages* 2020;1:85–88 CrossRef
20. Damiano RJ, Tutino VM, Paliwal N, et al. **Compacting a single flow diverter versus overlapping flow diverters for intracranial aneurysms: a computational study**. *AJNR Am J Neuroradiol* 2017;38:603–10 CrossRef Medline
21. Edelstein LC, Simon LM, Montoya RT, et al. **Racial differences in human platelet PAR4 reactivity reflect expression of PCTP and miR-376c**. *Nat Med* 2013;19:1609–16 CrossRef Medline
22. Xiang J, Tremmel M, Kolega J, et al. **Newtonian viscosity model could overestimate wall shear stress in intracranial aneurysm domes and underestimate rupture risk**. *J Neurointerv Surg* 2012;4:351–57 CrossRef Medline